Naval Research Laboratory

Washington, DC 20375-5320

Self-Magnetic Field Effects on Electron Emission as the Critical Current Is Approached

P. F. OTTINGER
G. COOPERSTEIN
J. W. SCHUMER

Pulsed Power Physics Branch
Plasma Physics Division

S. B. SWANEKAMP

JAYCOR, Inc.
McLean, VA

September 28, 2001

20011026 022

REPORT DOCUMENTATION PAGE

Public reporting burden for this collection of information is estimated to average 1 hour per response, including the time for reviewing instructions, searching existing data sources, gathering and maintaining the data needed, and completing and reviewing the collection of information. Send comments regarding this burden estimate or any other aspect of this collection of information, including suggestions for reducing this burden, to Washington Headquarters Services, Directorate for Information Operations and Reports, 1215 Jefferson Davis Highway, Suite 1204, Arlington, VA 22202-4302, and to the Office of Management and Budget, Paperwork Reduction Project (0704-0188), Washington, DC 20503.

1. AGENCY USE ONLY (*Leave Blank*)	2. REPORT DATE	3. REPORT TYPE AND DATES COVERED
	September 28, 2001	Interim

4. TITLE AND SUBTITLE

Self-Magnetic Field Effects on Electron Emission as the Critical Current Is Approached

5. FUNDING NUMBERS

6. AUTHOR(S)

P.F. Ottinger, G. Cooperstein, J.W. Schumer, and S.B. Swanekamp*

7. PERFORMING ORGANIZATION NAME(S) AND ADDRESS(ES)

Naval Research Laboratory
4555 Overlook Avenue, SW
Washington, DC 20375-5320

8. PERFORMING ORGANIZATION REPORT NUMBER

NRL/MR/6770--01-8567

9. SPONSORING/MONITORING AGENCY NAME(S) AND ADDRESS(ES)

Office of Naval Research, Arlington, VA
Department of Energy through
Sandia National Laboratories, Albuquerque, NM
Los Alamos National Laboratory, Albuquerque, NM
Lawrence Livermore National Laboratory, Livermore, CA

10. SPONSORING/MONITORING AGENCY REPORT NUMBER

11. SUPPLEMENTARY NOTES

*JAYCOR, Inc., McLean, VA 22102

12a. DISTRIBUTION/AVAILABILITY STATEMENT

Approved for public release; distribution is unlimited.

12b. DISTRIBUTION CODE

13. ABSTRACT (*Maximum 200 words*)

The self-magnetic field associated with the current in a planar diode is shown to reduce electron emission below the Child-Langmuir current density. As the magnetic field increases, the diode current is limited to the critical current. Here, a 1-D analysis is carried out to calculate the suppressed current density in the presence of a transverse magnetic field. The problem is shown to be similar to that of the limiting current (i.e., Hull current) calculated in a crossed field gap, in which a constant transverse magnetic field is applied across the gap to insulate the electron flow. In the case considered here, the magnetic field is produced by the diode current itself and this self-magnetic field decreases with distance along the gap. It is shown that the emitted current density is only modestly reduced from the Child-Langmuir current density. The 1-D analysis remains valid until critical current is approached, at which point orbit crossing occurs and a 2-D kinetic analysis is required. The minimum diode length required to reach critical current is also derived.

14. SUBJECT TERMS

Electron beam diodes

15. NUMBER OF PAGES

16

16. PRICE CODE

17. SECURITY CLASSIFICATION OF REPORT	18. SECURITY CLASSIFICATION OF THIS PAGE	19. SECURITY CLASSIFICATION OF ABSTRACT	20. LIMITATION OF ABSTRACT
UNCLASSIFIED	UNCLASSIFIED	UNCLASSIFIED	UL

TABLE OF CONTENTS

SELF-MAGNETIC FIELD EFFECTS ON ELECTRON EMISSION
AS THE CRITICAL IS APPROACHED

Abstract

The self-magnetic field associated with the current in a planar diode is shown to reduce electron emission below the Child-Langmuir current density. As the magnetic field increases, the diode current is limited to the critical current. Here, a 1-D analysis is carried out to calculate the suppressed current density in the presence of a transverse magnetic field. The problem is shown to be similar to that of the limiting current (i.e., Hull current) calculated in a crossed field gap, in which a constant transverse magnetic field is applied across the gap to insulate the electron flow. In the case considered here, the magnetic field is produced by the diode current itself and this self-magnetic field decreases with distance along the gap. It is shown that the emitted current density is only modestly reduced from the Child-Langmuir current density. The 1-D analysis remains valid until critical current is approached, at which point orbit crossing occurs and a 2-D kinetic analysis is required. The minimum diode length required to reach critical current is also derived.

I. Introduction

High power vacuum diodes are used to produce intense electron beams for many applications. When self-magnetic field effects are negligible and the cathode is a space-charge-limited (SCL) emitter, Child-Langmuir flow is obtained [1,2]. Here, cylindrical diodes are being considered with an anode-cathode gap that is much less than the diode radius. In this case, the problem can be treated as planar and, when the magnetic field is negligible, electrons cross the diode with straight-line trajectories as illustrated in Fig. 1a. However, when the self-magnetic field associated with the diode current becomes large enough to significantly deflect the electron path as it crosses the diode gap, the additional electron space charge density in the gap above the emission site reduces the emission below the Child-Langmuir current density. This situation is illustrated in Fig. 1b. At high magnetic field, the diode current is limited to the critical current I_{crit}, which is obtained when the electrons reach the anode at grazing incidence (or equivalently the "electron gyroradius" equals the gap size) [3,4]. Critical current flow is illustrated in Fig. 1c.

Here, a 1-D analysis is carried out to calculate the suppressed current density in the presence of a transverse magnetic field. The problem is shown to be similar to that of the limiting current (i.e., Hull current) calculated in a crossed field gap [5], in which a constant transverse magnetic field is applied across the gap to insulate the electron flow. In treating electron flow in crossed field gaps, the Llewellyn approach is typically

used [5], whereas here, Poisson's equation is solved by direct integration. Also, in the case considered here, the magnetic field is produced by the diode current itself and this self-magnetic field increases with distance along the gap causing the curvature of the electron trajectories to increase with distance as well (see Fig. 1c). It is shown that the emitted current density is only modestly reduced from the Child-Langmuir current density. The 1-D analysis remains valid until critical current is approached, at which point orbit crossing occurs and a 2-D kinetic analysis is required.

This problem is of interest for determining the minimum length of a diode designed to run at I_{crit}. This length will be defined as the critical length L_{crit}. This situation arises when an electron beam pinch is desired to concentrate the electron-beam energy, while minimizing losses to ion current. If anode plasma forms, ion current is generated and its magnitude is proportional to the diode length in cylindrical diodes (or diode radius in pinched-beam diodes)[6-10]. Thus, minimizing the diode length minimizes the current lost to ions. Although this analysis does not include ion current, a reasonable estimate of the desired minimum diode length with ion current is easily obtained. For a nonrelativistic planar diode, it is well known that the SCL electron current density is enhanced by a constant factor of 1.86 when ion current is included in the analysis[11]. The scaling of the current density with diode voltage and gap are the same in bipolar flow with ions as it is when only electron current flows. Thus, it is assumed here that the minimum diode length for bipolar flow L_{crit}^{BP} is to first order simply a factor of 1.86 smaller than the minimum length without ions (i.e., $L_{crit}^{BP} = L_{crit}/1.86$).
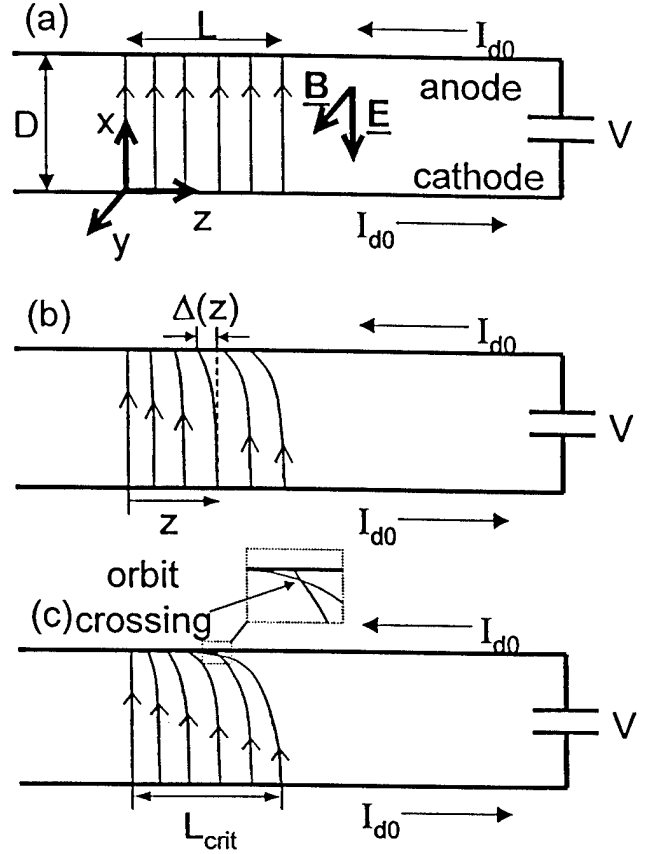

Figure 1. Schematic of electron flow accelerated by the electric field E across a diode with a transverse self-magnetic field B that is generated by the diode current. Here, V is the diode voltage, I_{d0} is the total diode current, D is the diode anode-cathode gap spacing, and L is the length of the diode emission area. The thin arrows indicate the electron trajectories (a) for $I_{d0} \ll I_{crit}$, (b) for $I_{d0} < I_{crit}$, and (c) for $I_{d0} = I_{crit}$. $\Delta(z)$ is the axial distance an electron is deflected by the local transverse magnetic field while crossing the gap.

In Sec. II of this paper, a 1-D analysis is carried out to calculate the electron current density as a function of the transverse magnetic field. The results of this analysis are then applied in Sec. III to find the current as a function of distance along a diode. By

equating this current to I_{crit}, the critical length is obtained. Finally, the results of this work are summarized in Sec. IV.

II. Electron current density as a function of the transverse magnetic field

The planar diode geometry considered here is illustrated in Fig.1. A voltage V is applied across the electrodes that are separated by a distance D. For this part of the analysis, a uniform magnetic field is applied transverse to the electron flow in the y direction and current is emitted over an axial length L as shown in Fig. 1a. For this situation, the electric potential $\Phi(x)$ and the magnetic vector potential $A_z(x)$ can be written as

$$\frac{d\Phi(x)}{dx} = -E_x(x) \quad , \tag{1}$$

$$A_z(x) = -B_0 x \quad , \tag{2}$$

where E_x is the electric field in the gap, the constant magnetic field $B_0 > 0$, $\Phi(0) = 0$, and $\Phi(D) = V$. For SCL flow, an additional boundary condition is $E_x(0) = d\Phi/dx(0) = 0$. In equilibrium, the continuity equation requires that the current density $J_x(x)$ be given by

$$J_x(x) = -J_0 \quad , \tag{3}$$

where again the constant $J_0 > 0$. Because y and z are ignorable coordinates, the canonical momentum associated with each of these coordinates is conserved. Thus, the velocity components $v_y(x)$ and $v_z(x)$ of the electrons can be written as

$$v_y(x) = 0 \quad , \tag{4}$$

$$v_z(x) = -\omega_{ce}x \quad , \tag{5}$$

where $\omega_{ce} = eB_0/m_e c$, e is the electron charge, m_e is the electron mass, c is the speed of light, and it is assumed that the electrons are born on the cathode surface at $x = 0$ with zero energy. Using this same assumption, an expression for $v_x(x)$ is obtained from conservation of energy,

$$v_x^2(x) = \frac{2e\Phi(x)}{m_e} - \omega_{ce}^2 x^2 \quad . \tag{6}$$

Here, Eqs. (4) and (5) have been used to substitute for v_y and v_z.

Equation (6) immediately provides an expression for the critical current I_{crit}. Because $v_x^2 \geq 0$ is required for a physically meaningful result from Eq. (6), the current I must be less than or equal to I_{crit}, where

$$I_{crit} = \left(\frac{m_e c^4}{2e}\right)^{1/2} V^{1/2} \frac{R}{D} \quad , \tag{7}$$

and

$$B_0 \equiv \frac{2I}{Rc} \quad . \tag{8}$$

Note that B_0 is defined as in Eq. (8) so that these 1D results can be related to problems in cylindrical geometry with R >> D, where R is the cathode radius. From Eqs. (7) and (8), the critical magnetic field is found to be $B_0^{crit} = 2I_{crit}/Rc$. The critical current is also referred to as the Hull current for systems where B_0 is applied [5].

An equation for $\Phi(x)$ can now be obtained. Using Eq. (3) and $J_x = -en_ev_x$ to write the electron density as

$$n_e(x) = \frac{J_0}{ev_x(x)} \quad , \tag{9}$$

Poisson's equation becomes

$$\frac{d^2\Phi}{dx^2} = \frac{4\pi J_0}{\sqrt{\frac{2e\Phi}{m_e} - \omega_{ce}^2 x^2}} \quad . \tag{10}$$

The solution to this equation that satisfies the boundary conditions ($\Phi(0) = 0$, $\Phi(D) = V$, and $d\Phi/dx(0) = 0$) provides a complete solution to the problem by substituting $\Phi(x)$ back into Eqs. (1), (6), and (9) for $E_x(x)$, $v_x(x)$, and $n_e(x)$ respectively. In addition, $v_y(x)$ and $v_z(x)$ are given by Eqs. (4) and (5). Because Eq. (10) is a second-order differential equation, it requires only two boundary conditions. The third boundary condition determines the eigenvalue for J_0.

In order to solve Eq. (10), it is convenient to rewrite the equation as

$$\frac{d^2S}{dx^2} = \frac{8\pi eJ_0}{m_e\sqrt{S}} - 2\omega_{ce}^2 \quad , \tag{11}$$

where

$$S = v_x^2 \quad , \tag{12}$$

and v_x^2 is given in terms of $\Phi(x)$ and x in Eq. (6). The first integral can be obtained by multiplying both sides of the equation by dS/dx and integrating. This yields

$$\frac{dS}{dx} = \pm\left(\frac{32\pi eJ_0}{m_e}\sqrt{S} - 4\omega_{ce}^2 S\right)^{1/2} \quad , \tag{13}$$

where $S(0) = 0$ and $dS/dx(0) = 0$ have been used. These new boundary conditions can be derived from the boundary conditions on Φ at $x = 0$, and Eqs. (12) and (6). Because S is associated with v_x^2 [see Eq. (12)], the upper sign applies in the usual case when v_x is increasing, while the lower sign applies when v_x is decreasing. Note that v_x will only decrease if the electron orbit has been significantly deflected by the magnetic field so that energy is being transferred into axial motion. This occurs when I approaches I_{crit}.

The second integral can be obtained by directly integrating Eq. (13) and using the boundary condition $S(0) = 0$. Using Eqs. (6) and (12) to write the solution in terms of $\Phi(x)$, yields for $dS/dx > 0$ [i.e., the upper sign in Eq. (13)]

$$x = -\left[\frac{8\pi eJ_0}{m_e\omega_{ce}^4}\left(\frac{2e\Phi(x)}{m_e} - \omega_{ce}^2 x^2\right)^{1/2} - \frac{1}{\omega_{ce}^2}\left(\frac{2e\Phi(x)}{m_e} - \omega_{ce}^2 x^2\right)\right]^{1/2}$$
$$+ \frac{4\pi eJ_0}{m_e\omega_{ce}^3}\left\{Sin^{-1}\left[\frac{m_e\omega_{ce}^2}{4\pi eJ_0}\left(\frac{2e\Phi(x)}{m_e} - \omega_{ce}^2 x^2\right)^{1/2} - 1\right] + \frac{\pi}{2}\right\} \quad . \tag{14}$$

This solution only applies for $x < x^{(1)}$ where $x^{(1)}$ is defined below [see Eq. (24)] as the position where v_x stops increasing (i.e., where $dS/dx = 0$). The value of $x^{(1)}$ depends on the magnetic field strength through ω_{ce}. When $x^{(1)} > D$, Eq. (14) applies for all $0 \le x \le D$. When $x^{(1)} \le D$, Eq. (14) applies for $0 \le x \le x^{(1)}$ and Eq. (13) must be solved again using the lower sign this time for $x^{(1)} \le x \le D$ and that solution matched to the solution in Eq. (14) at $x = x^{(1)}$. This solution is found below [see Eq. (26)]. Assuming for now that $x^{(1)} > D$, the boundary condition $\Phi(D) = V$ can be applied to Eq. (14) to provide a transcendental equation for the eigenvalue J_0 for a given value of ω_{ce}. Once $J_0(\omega_{ce})$ is determined, Eq. (14) can be solved numerically for $\Phi(x)$.

It is instructive to examine this solution for small values of B_0. To accomplish this, let

$$\varepsilon \equiv \frac{m_e \omega_{ce}^2}{4\pi e J_0}\left(\frac{2e\Phi(x)}{m_e} - \omega_{ce}^2 x^2\right)^{1/2} \ll 1 \qquad . \tag{15}$$

Using the expansion

$$\mathrm{Sin}^{-1}(\varepsilon - 1) = -\frac{\pi}{2} + (2\varepsilon)^{1/2} + \frac{\varepsilon^{3/2}}{6\sqrt{2}} + \frac{7\varepsilon^{5/2}}{144\sqrt{2}} + ... \qquad \text{for } \varepsilon \ll 1 \qquad , \tag{16}$$

Eq. (14) can be expanded to give

$$x = \left(\frac{m_e}{18\pi e J_0}\right)^{1/2}\left(\frac{2e\Phi(x)}{m_e} - \omega_{ce}^2 x^2\right)^{3/4}\left[1 + \frac{m_e \omega_{ce}^2}{24\pi e J_0}\left(\frac{2e\Phi(x)}{m_e} - \omega_{ce}^2 x^2\right)^{1/2} + ...\right] \qquad . \tag{17}$$

First, note that, for $B_0 = 0$ (i.e., $\omega_{ce} = 0$), the Child-Langmuir equation is recovered. To obtain this result, the final boundary condition, $\Phi(D) = V$, is applied yielding

$$J_0^{(0)} = J_{CL} \equiv \frac{1}{9\pi}\left(\frac{2e}{m_e}\right)^{1/2}\frac{V^{3/2}}{D^2} \qquad . \tag{18}$$

Here, $J_0^{(0)}$ is defined as the value for J_0 at $\omega_{ce} = 0$. Equation (17) can also be manipulated to find an iterative solution for J_0 with $x = D$ and $\Phi(D) = V$. Retaining only the first two terms gives

$$J_0 = \frac{1}{9\pi}\left(\frac{2e}{m_e}\right)^{1/2}\frac{\left(V - \frac{m_e \omega_{ce}^2 D^2}{2e}\right)^{3/2}}{D^2}\left[1 + \frac{3m_e \omega_{ce}^2 D^2/4e}{\left(V - \frac{m_e \omega_{ce}^2 D^2}{2e}\right)} + ...\right] \qquad . \tag{19}$$

This expansion is the Child-Langmuir current corrected for the presence of the small magnetic field, which, as expected, reduces J_0 below J_{CL}. Although the leading terms in the expansion shown in Eq. (19) vanish as $I \to I_{crit}$, the higher order terms in the expansion that are not shown diverge as $I \to I_{crit}$ because

$$\omega_{ce}^2 \to (\omega_{ce}^{crit})^2 \equiv \frac{2eV}{m_e D^2} \qquad . \tag{20}$$

Thus, Eq. (19) is only valid for $\omega_{ce} < \omega_{ce}^{crit}$.

As the magnetic field strength increases, a point is reached where the electron orbit has been deflected axially so much that v_x begins to decrease before the electron reaches the anode. In fact, for $\omega_{ce} = \omega_{ce}^{crit}$, the electron slows down in the x direction to the point that $v_x = 0$ when the electron reaches the anode. When v_x stops increasing, $dS/dx = 0$, and when v_x begins to decrease, the lower sign in Eq. (13) applies. To find the magnetic field strength where the electron reaches the anode just as the electron stops accelerating the x direction, Eq. (13) is solved at $x = D$ (and $\Phi(D) = V$) with $dS/dx = 0$. This yields

$$\frac{8\pi e J_0^{(1)}}{m_e} = \left(\omega_{ce}^{(1)}\right)^2 \left[\frac{2eV}{m_e} - \left(\omega_{ce}^{(1)}\right)^2 D^2\right]^{1/2} \quad , \tag{21}$$

where $\omega_{ce}^{(1)}$ denotes the magnetic field strength where $dS/dx = 0$ at $x = D$ and $J_0^{(1)}$ is the current density for this special magnetic field strength. This result can be substituted into Eq. (14) to obtain an expression for $J_0^{(1)}$ with $\omega_{ce} = \omega_{ce}^{(1)}$. Substituting this result back into Eq. (21) and solving for $\omega_{ce}^{(1)}$ yields for $x^{(1)} = D$

$$\omega_{ce}^{(1)} = \frac{\pi}{\left(\pi^2 + 4\right)^{1/2}} \left(\frac{2eV}{m_e D^2}\right)^{1/2} = \frac{\pi \omega_{ce}^{crit}}{\left(\pi^2 + 4\right)^{1/2}} \approx 0.844 \omega_{ce}^{crit} \quad , \tag{22}$$

and

$$J_0^{(1)} = \frac{m_e D}{4\pi^2 e} \left(\omega_{ce}^{(1)}\right)^3 = \frac{9\pi^2 J_{CL}}{2\left(\pi^2 + 4\right)^{3/2}} \approx 0.86 J_{CL} \quad . \tag{23}$$

Thus, for $0 \le \omega_{ce} \le \omega_{ce}^{(1)}$, Eq. (14) applies and J_0 decreases from J_{CL} at $\omega_{ce} = 0$ to $0.86 J_{CL}$ at $\omega_{ce} = \omega_{ce}^{(1)}$.

For $\omega_{ce}^{(1)} < \omega_{ce} \le \omega_{ce}^{crit}$, the problem is more complicated. Equation (14) applies for $0 \le x \le x^{(1)}$ where $x^{(1)}$ is defined to be the position where $dS/dx = 0$ (i.e., where v_x begins to decrease). However, for $x^{(1)} \le x \le D$, Eq. (13) must be solved again using the lower sign and then this new solution must be matched to Eq. (14) at $x = x^{(1)}$. An expression for $x^{(1)}$ can be found by equating the right hand side (RHS) of Eq. (13) to zero and substituting the resulting value of $S(x^{(1)})$ into Eq. (14) evaluated at $x = x^{(1)}$. This procedure yields

$$x^{(1)} = \frac{4\pi^2 e J_0}{m_e \omega_{ce}^3} \quad , \tag{24}$$

and

$$S(x^{(1)}) = \left(\frac{8\pi e J_0}{m_e \omega_{ce}^2}\right)^2 \quad , \tag{25}$$

where J_0 is a function of ω_{ce} and is yet to be determined. The matching condition at $x^{(1)}$ can then be used to give

$$x = +\left[\frac{8\pi e J_0}{m_e \omega_{ce}^4}\left(\frac{2e\Phi(x)}{m_e} - \omega_{ce}^2 x^2\right)^{1/2} - \frac{1}{\omega_{ce}^2}\left(\frac{2e\Phi(x)}{m_e} - \omega_{ce}^2 x^2\right)\right]^{1/2}$$

$$- \frac{4\pi e J_0}{m_e \omega_{ce}^3}\left\{\text{Sin}^{-1}\left[\frac{m_e \omega_{ce}^2}{4\pi e J_0}\left(\frac{2e\Phi(x)}{m_e} - \omega_{ce}^2 x^2\right)^{1/2} - 1\right] - \frac{3\pi}{2}\right\} \quad , \tag{26}$$

for $x^{(1)} \leq x \leq D$ and $\omega_{ce}^{(1)} < \omega_{ce} \leq \omega_{ce}^{crit}$. Applying the boundary condition $\Phi(D) = V$ at $x = D$ to Eq. (26) provides a transcendental equation for the eigenvalue J_0 for a given value of ω_{ce}. Note that, for the special case of $\omega_{ce} = \omega_{ce}^{crit}$, J_0 is defined as J_0^{crit} which, from Eqs. (18), (20), and (26), is found to be

$$J_0^{crit} = \frac{9J_{CL}}{4\pi} \approx 0.716 J_{CL} \quad . \tag{27}$$

Once J_0 is determined as a function of ω_{ce}, Eqs. (14) and (26) can be solved numerically for $\Phi(x)$ as a function of ω_{ce}.

In order to examine the behavior of the solution near $\omega_{ce} = \omega_{ce}^{crit}$, Eq. (26) can be expand about $x = D$ using the same small parameter ε as defined in Eq. (15). Here, ε is small because $2e\Phi/m_e \sim \omega_{ce}^2 x^2$ for $\omega_{ce} \sim \omega_{ce}^{crit}$ and $x \sim D$. As done with J_0 for $\omega_{ce} \sim 0$ in Eq. (19), this expansion can also be manipulated to find an iterative solution for J_0 with $x = D$ and $\Phi(D) = V$ for $\omega_{ce} \sim \omega_{ce}^{crit}$. Retaining only the first two terms gives

$$J_0 = \frac{9J_{CL}}{4\pi}\left[1 + \frac{4}{3}\left(\frac{\pi^2}{2}\right)^{1/4}\left(1 - \frac{\omega_{ce}}{\omega_{ce}^{crit}}\right)^{3/4} - 3\left(1 - \frac{\omega_{ce}}{\omega_{ce}^{crit}}\right) + ...\right] \quad , \tag{28}$$

where Eq. (27) is recovered for $\omega_{ce} = \omega_{ce}^{crit}$. Note that, as $\omega_{ce} \rightarrow \omega_{ce}^{crit}$, the derivative of J_0 with respect to ω_{ce} diverges as

$$\frac{\partial J_0}{\partial \omega_{ce}} = -\frac{9J_{CL}}{4\pi\omega_{ce}^{crit}}\left(\frac{\pi^2}{2}\right)^{1/4}\left(1 - \frac{\omega_{ce}}{\omega_{ce}^{crit}}\right)^{-1/4} + ... \rightarrow -\infty \quad . \tag{29}$$

Thus, the electron emission abruptly shuts off at $\omega_{ce} = \omega_{ce}^{crit}$.

A numerical solution of the transcendental equation for J_0 has been obtained for all values of ω_{ce} in the range $0 < \omega_{ce} \leq \omega_{ce}^{crit}$. For $0 < \omega_{ce} \leq \omega_{ce}^{(1)}$, the transcendental equation given in Eq. (14) is used with $\Phi = V$ and $x = D$, while, for $\omega_{ce}^{(1)} < \omega_{ce} \leq \omega_{ce}^{crit}$, Eq. (26) is used with the same boundary conditions. A plot of J_0 as a function of ω_{ce} is shown in Fig. 2 as the solid curve. As expected from the above results, the current density decreases slowly with magnetic field until ω_{ce}^{crit} is reached where emission abruptly shuts off. The approximation for J_0 given in Eq. (19) is also plotted in Fig. 2 as the dashed curve. This approximation is only reasonably accurate for < 0.7. Retaining additional terms in the expansion would extend the accuracy of the approximation to larger $\omega_{ce}/\omega_{ce}^{crit}$ but the additional terms would diverge at $\omega_{ce}/\omega_{ce}^{crit} = 1$. Note that retaining only the first term in the expansion given in Eq. (19), provides an approximation that is only

accurate for very small $\omega_{ce}/\omega_{ce}^{crit}$ (see dotted curve in Fig. 2). A plot of $x^{(1)}/D$ as a function of ω_{ce} is also plotted in Fig. 2 where $x^{(1)} \leq D$.

Using the solution for J_0 shown in Fig. 2, Eqs. (14) and (26) can be used to solve for $\Phi(x)$ for a given value of ω_{ce}. Equations (6), (5), and (9) can then be used to obtain $v_x(x)$, $v_z(x)$, and $n_e(x)$, respectively for a given value of ω_{ce}. Solutions for $\Phi(x)$, $n_e(x)$, $v_x(x)$, and $v_z(x)$ are plotted in Figs. 3 – 6 respectively for cases with $\omega_{ce}/\omega_{ce}^{crit}$ = 0, 0.25, 0.5, 0.75, and 1.0. In these plots, $v_x(x)$, and $v_z(x)$ are normalized to v_0 = $(2eV/m_e)^{1/2}$, and $n_e(x)$ is normalized to $n_0 = n_e(D)$ for $\omega_{ce}/\omega_{ce}^{crit}$ = 0. From Eq. (18), $n_0 = J_{CL}/ev_0 = V/(9\pi e D^2)$. The profile of the potential $\Phi(x)$ does not vary much as $\omega_{ce}/\omega_{ce}^{crit}$
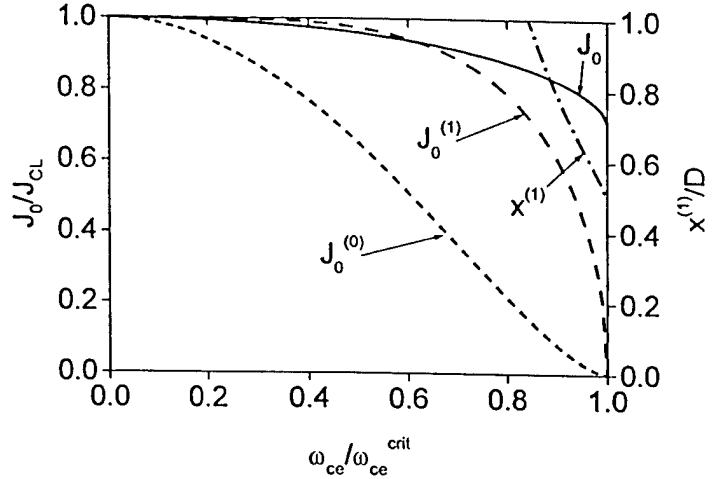

Figure 2. Plots of the normalized electron current density J_0/J_{CL} (solid) and the normalized distance $x^{(1)}/D$ for $x^{(1)} \leq D$ (dot-dash) as functions of the normalized transverse magnetic field strength $\omega_{ce}/\omega_{ce}^{crit} = B_0/B_0^{crit}$. Also shown are plots of $J_0^{(0)}$ (dot), the zero order approximation to J_0 from the first term in Eq. (19), and $J_0^{(1)}$ (dash), the first order approximation to J_0 from the first two terms in Eq. (19).
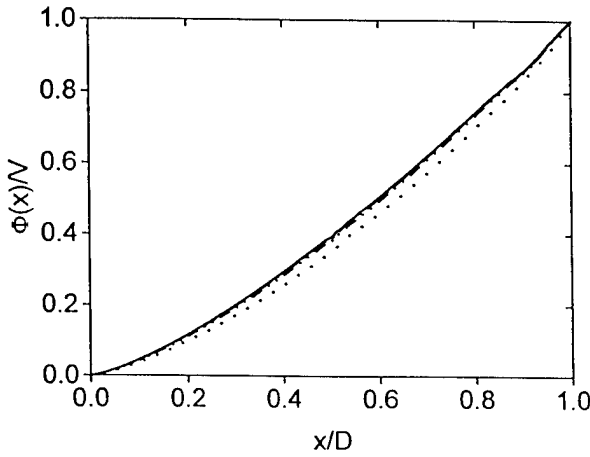

Figure 3. Plots of the normalized potential $\Phi(x)/V$ as a function of the normalized distance across the gap x/D for various values of $\omega_{ce}/\omega_{ce}^{crit}$. Plots for $\omega_{ce}/\omega_{ce}^{crit}$ = 0.0 (solid), 0.25 (dash), 0.5 (dash-dot), and 0.75 (dash-dot-dot) nearly lay on top of each other, while the plot for $\omega_{ce}/\omega_{ce}^{crit}$ = 1.0 (dot) lies slightly below the other curves.
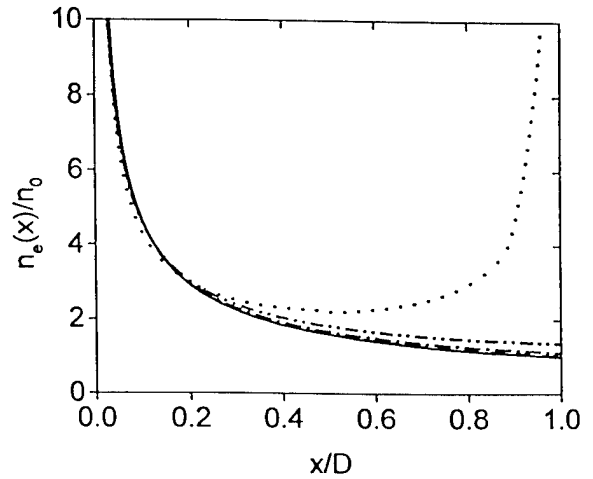

Figure 4. Plots of the normalized density n_e/n_0 as a function of the normalized distance across the gap x/D for various values of $\omega_{ce}/\omega_{ce}^{crit}$. Plots for $\omega_{ce}/\omega_{ce}^{crit}$ = 0.0 (solid), 0.25 (dash), 0.5 (dash-dot), and 0.75 (dash-dot-dot) nearly lay on top of each other, while the plot for $\omega_{ce}/\omega_{ce}^{crit}$ = 1.0 (dot) diverges as it approaches the anode at $x = D$.
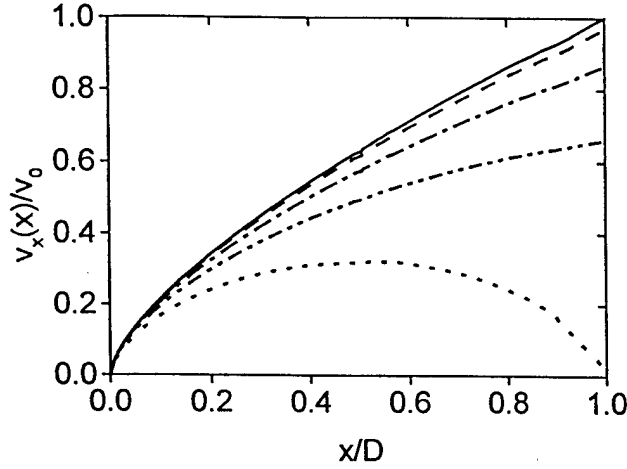
Figure 5. Plots of the normalized velocity v_x/v_0 as a function of the normalized distance across the gap x/D for various values of $\omega_{ce}/\omega_{ce}^{crit}$. Plots are shown for $\omega_{ce}/\omega_{ce}^{crit}$ = 0.0 (solid), 0.25 (dash), 0.5 (dash-dot), 0.75 (dash-dot-dot), and 1.0 (dot).
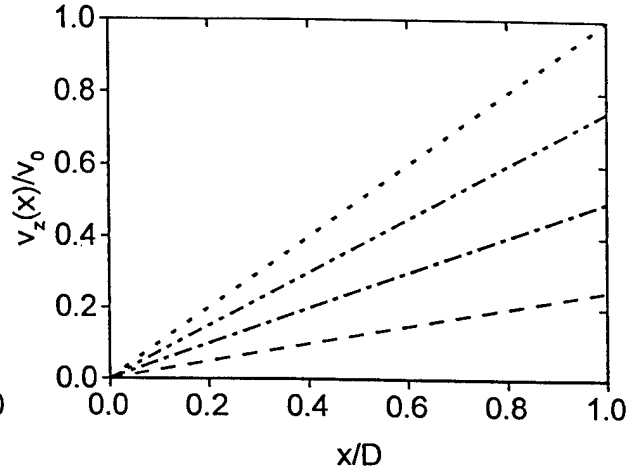
Figure 6. Plots of the normalized velocity v_z/v_0 as a function of the normalized distance across the gap x/D for various values of $\omega_{ce}/\omega_{ce}^{crit}$. Plots are shown for $\omega_{ce}/\omega_{ce}^{crit}$ = 0.0 (solid), 0.25 (dash), 0.5 (dash-dot), 0.75 (dash-dot-dot), and 1.0 (dot).

increases with four of the five curves lying nearly on top of each other and the $\omega_{ce}/\omega_{ce}^{crit}$ = 1 curve lying only slightly below the other curves. The density profile $n_e(x)$ is also little changed over most of the range for $\omega_{ce}/\omega_{ce}^{crit}$ but changes dramatically as $\omega_{ce}/\omega_{ce}^{crit}$ approaches unity where the density diverges at the anode. The profiles of the electron velocity components $v_x(x)$ and $v_z(x)$ both depend strongly on $\omega_{ce}/\omega_{ce}^{crit}$. For $\omega_{ce}/\omega_{ce}^{crit}$ = 1, note that $v_x(x)$ goes to zero as the electrons approach the anode at grazing incidence.

III. Minimum diode length for obtaining critical current

If laminar flow is assumed in the diode gap, then the above analysis can be used to calculate the diode current $I_d(z)$ as a function of distance along the cathode. The total current in the diode is I_{d0} as shown in Fig. 1. $I_d(z)$ increases from zero at z = 0 to I_{d0} at z = L. Following the notation used in Eq. (8), the local self-magnetic field associated with this diode current is given by

$$B_0(z) = \frac{2I_d(z)}{Rc} \quad , \tag{30}$$

and determines the local current density from J_0 as a function of B_0 given in Fig. 2. Here, this local current density is denoted by $J_0(z)$ and $dI_d(z)/dz \equiv 2\pi R J_0(z)$. This diode configuration is illustrated in Fig. 1a for $I_{d0} \ll I_{crit}$, in Fig. 1b for $I_{d0} < I_{crit}$, and in Fig. 1c for $I_{d0} = I_{crit}$. This analysis, which assumes that z is an ignorable coordinate, is still approximately correct as long as variations in the z direction are small compared to variations in the x direction (i.e., d/dz << d/dx). This is supported by the fact that $J_0(z)$ only varies slowly with $B_0(z)$ as shown in Fig. 2.

The minimum diode length needed to obtain critical current then is determined by

$$I_d(L_{crit}) \equiv 2\pi R \int_0^{L_{crit}} J_0(z)dz = I_{crit} \qquad ,$$ (31)

where I_{crit} is defined in Eq. (7). Because J_0 decreases slowly with $\omega_{ce}/\omega_{ce}^{crit}$ (i.e., with B_0), a zero order estimate (and lower bound) for L_{crit} can be obtained by assuming that $J_0(z)$ is uniform in z and equal to J_{CL}, yielding

$$L_{crit}^0 = \frac{9D}{2\beta^2} \qquad .$$ (32)

Here, $\beta = v_0/c$. Note that $L_{crit}^0 \gg D$ for nonrelativistic beams, and that $L_{crit}^0 \to 9D/2$ as $\beta \to 1$ where this nonrelativistic analysis breaks down. Using L_{crit}^0 to scale z, Eq. (31) can be integrated to solve for L_{crit}. The results are plotted in Fig. 7 and show that

$$L_{crit} = 1.076 L_{crit}^0 \qquad .$$ (33)

This provides both scaling for and a reasonable estimate of the minimum diode length required for critical current.

To examine the validity of the laminar flow assumption, consider the distance $\Delta(z)$ that an electron is deflected axially while traversing the diode gap as illustrated in Fig. 1b. At z = 0, the self-magnetic field vanishes so $\Delta(0) = 0$. For z > 0, $\Delta(z)$ monotonically increases and can be written as

$$\Delta(z) \equiv \int_0^T v_z(x)dt = \int_0^D \frac{v_z}{v_x}dx \qquad ,$$ (34)

where T is the transit time of the electron for crossing the diode gap D, and v_z and v_x are defined in Eqs. (5) and (6) respectively. Noting that the denominator of the integrand is just $v_x = S^{1/2}$ [see Eq. (12)] and that Eqs. (14) and (26) can be used to write $v_z(x) = \omega_{ce}x$ in terms of S, Eq. (34) can be rewritten as an integral in S where from Eq. (13)

$$dx = \pm\left(\frac{32\pi e J_0}{m_e}\sqrt{S} - 4\omega_{ce}^2 S\right)^{-1/2} dS \qquad .$$ (35)

When $0 \le \omega_{ce} \le \omega_{ce}^{(1)}$, Eq. (14) is used to substitute into Eq. (34) for x to write the integral in terms of S. When $\omega_{ce}^{(1)} < \omega_{ce} \le \omega_{ce}^{crit}$, the integral must be broken into two parts; for $0 \le x \le x^{(1)}$, Eq. (14) is used to substitute for x in terms of S, and for $x^{(1)} \le x \le D$, Eq. (26) is used. Performing the integration yields

$$\Delta(z) = \frac{-1}{\omega_{ce}}\left(\frac{2eV}{m_e} - \omega_{ce}^2 D^2\right)^{1/2} + \frac{2\pi^2 e J_0}{m_e \omega_{ce}^3} Sin^{-1}\left[\frac{m_e \omega_{ce}^2}{4\pi e J_0}\left(\frac{2eV}{m_e} - \omega_{ce}^2 D^2\right)^{1/2} - 1\right]$$

$$+ \frac{\pi e J_0}{m_e \omega_{ce}^3}\left(\frac{\pi^2}{2} + 2\left\{Sin^{-1}\left[\frac{m_e \omega_{ce}^2}{4\pi e J_0}\left(\frac{2eV}{m_e} - \omega_{ce}^2 D^2\right)^{1/2} - 1\right]\right\}^2\right)$$ (36)

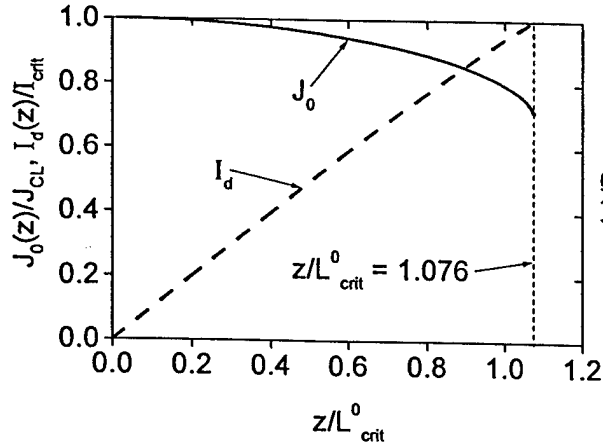for $0 \le \omega_{ce} \le \omega_{ce}^{(1)}$, and

Figure 7. Plots of the normalized current density $J_0(z)/J_{CL}$ (solid) and the normalized diode current $I_d(z)/I_{crit}$ (dash) as functions of the normalized distance along the diode z/L^0_{crit}.
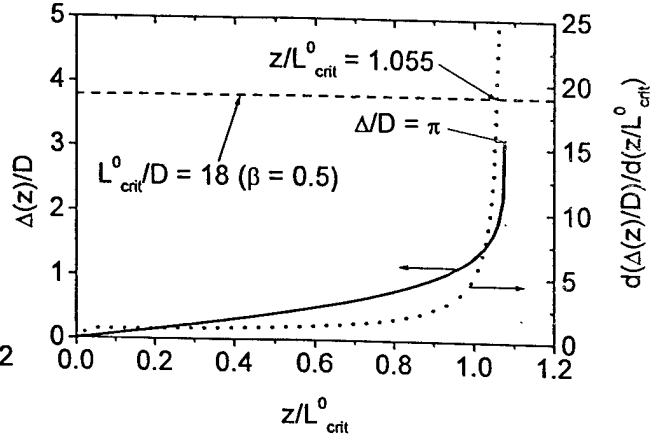
Figure 8. Plots of the normalized axial deflection of an electron $\Delta(z)/D$ (solid) as it crosses the gap and the normalized derivative of the axial deflection $d(\Delta(z)/D)/d(z/L^0_{crit})$ (dash) as functions of the normalized distance along the diode z/L^0_{crit}.

$$\Delta(z) = \frac{-1}{\omega_{ce}}\left(\frac{2eV}{m_e} - \omega_{ce}^2 D^2\right)^{1/2} - \frac{6\pi^2 e J_0}{m_e \omega_{ce}^3}\text{Sin}^{-1}\left[\frac{m_e \omega_{ce}^2}{4\pi e J_0}\left(\frac{2eV}{m_e} - \omega_{ce}^2 D^2\right)^{1/2} - 1\right]$$

$$+ \frac{\pi e J_0}{m_e \omega_{ce}^3}\left(\frac{9\pi^2}{2} + 2\left\{\text{Sin}^{-1}\left[\frac{m_e \omega_{ce}^2}{4\pi e J_0}\left(\frac{2eV}{m_e} - \omega_{ce}^2 D^2\right)^{1/2} - 1\right]\right\}^2\right) \tag{37}$$

for $\omega_{ce}^{(1)} < \omega_{ce} \leq \omega_{ce}^{crit}$. In Eqs. (36) and (37), the z dependence appears on the RHS through $J_0(z)$ and $\omega_{ce}(z) = eB_0(z)/m_e c$, where the explicit dependence on z has been suppressed for the sake of brevity. Note that Eqs. (36) and (37) can be written in dimensionless form by using the normalized parameters $\Delta(z)/D$, J_0/J_{CL}, and $\omega_{ce}(z)/\omega_{ce}^{crit}$.

The orbit of an electron emitted from the cathode at $z + \delta$ crosses the orbit of an electron emitted at z if $z - \Delta(z) > (z + \delta) - \Delta(z + \delta)$. In the limit of $\delta \ll z$, the last term on the RHS of this equation can be Taylor expanded. Upon substitution of this expansion, the leading terms in the orbit crossing condition cancel. Thus, in the limit of $\delta \to 0$, the criteria for orbit crossing simply becomes

$$\frac{d\Delta}{dz} > 1 \tag{38}$$

In order to evaluate Eq. (38), expressions for dJ_0/dz and $d\omega_{ce}/dz$ are needed. First note that $dJ_0/dz = (dJ_0/d\omega_{ce})d\omega_{ce}/dz$ where the solution for $J_0(\omega_{ce})$ is shown in Fig. 2 and its differentiation with respect to ω_{ce} is straight forward. Then note that $d\omega_{ce}/dz = (2e/m_e Rc^2)dI_d/dz = 4\pi e J_0(z)/m_e c^2$ where $I_d(z)$ and $J_0(z)$ are shown in Fig. 7. Plots of $\Delta(z)$

and $d\Delta(z)/dz$ are shown in Fig. 8 where $\Delta(z)$ has been normalized to D and z has been normalized to L^0_{crit}. With this normalization Eq. (38) becomes

$$\frac{d(\Delta(z)/D)}{d(z/L^0_{crit})} > \frac{L^0_{crit}}{D} = \frac{9}{2\beta^2} \qquad (39)$$

Thus, as the voltage increases (where $\beta^2 \sim V$), the location where orbit crossing first occurs moves to smaller z. The case with $\beta = 0.5$ (i.e., V = 64 kV) yields $L^0_{crit}/D = 18$ and is shown as an example in Fig. 8. For this case, orbit crossing first occurs at $z \sim 1.055 L^0_{crit}$. Because orbit crossing only occurs very close to $L_{crit} = 1.076\ L^0_{crit}$, the analysis is valid over nearly the full diode length and Eq. (33) provides an accurate estimate for L_{crit}.

IV. Conclusions

The self-magnetic field associated with the diode current in a planar diode is shown to reduce electron emission below the Child-Langmuir current density. As the magnetic field increases, the diode current is limited to the critical current I_{crit}. This problem is of interest for determining the minimum length L_{crit} of a diode designed to run at I_{crit}. This situation arises when an electron beam pinch is desired to concentrate the electron-beam energy, while minimizing losses to ion current. If anode plasma forms, ion current is generated and its magnitude is proportional to the diode length. Thus, minimizing the diode length minimizes the current lost to ions. Here, a 1-D analysis is carried out to calculate the suppressed electron current density in the presence of a transverse magnetic field without ions. The problem is shown to be similar to that of the limiting current (i.e., Hull current) calculated in a crossed field gap, in which a constant transverse magnetic field is applied across the gap to insulate the electron flow. In treating electron flow in crossed field gaps, the Llewellyn approach is typically used, whereas here, Poisson's equation is solved by direct integration. Also, in the case considered here, the magnetic field is produced by the diode current itself and this self-magnetic field varies with distance along the gap. Special values of some of the important parameters are listed in Table 1.

Table 1. Special values for various important parameters. Note that
$J_{CL} = (2e/m_e)^{1/2} V^{3/2}/9\pi D^2$, $v_0 = (2eV/m_e)^{1/2}$, $\omega^{crit}_{ce} = v_0/D$, and $n_0 = J_{CL}/ev_0$.

	$\omega_{ce} = 0$	$\omega_{ce} = \omega_{ce}^{(1)}$	$\omega_{ce} = \omega_{ce}^{crit}$
$\omega_{ce}/\omega_{ce}^{crit}$	0	$\pi/(\pi^2 + 4)^{1/2} \sim 0.84$	1
J_0/J_{CL}	1	$9\pi^2/2(\pi^2 + 4)^{3/2} \sim 0.86$	$9/4\pi \sim 0.72$
$x^{(1)}/D$	$+\infty$	1	0.5
$n_e(D)/n_0$	1	$9\pi^2/4(\pi^2 + 4) \sim 1.6$	$+\infty$
$v_x(D)/v_0$	1	$2/(\pi^2 + 4)^{1/2} \sim 0.54$	0
$v_z(D)/v_0$	0	$-\pi/(\pi^2 + 4)^{1/2} \sim -0.84$	-1
$\Delta(D)/D$	0	$(\pi^2 - 4)/2\pi \sim 0.93$	π

It is shown that the emitted current density is only modestly reduced from the Child-Langmuir current density J_{CL} with the current density only dropping to $0.716J_{CL}$ at I_{crit}. Application of the 1-D analysis to the pinched beam diode remains valid until critical current is approached, at which time orbit crossing occurs and a 2-D kinetic analysis is required. However, it is shown that orbit crossing only occurs very close to the end of the pinched beam diode. Thus, a reasonable estimate for the critical-current diode length is $L_{crit} = 1.076L^0_{crit} = 4.84D/\beta^2$. Although this analysis does not include ion current, an argument is made for extending these results for the case with ions. For a nonrelativistic planar diode, it is well known that the SCL electron current density is enhanced by a constant factor of 1.86 when ion current is included in the analysis. The scaling of the current density with diode voltage and gap are the same in bipolar flow with ions as it is when only electron current flows. Thus, it is assumed here that the minimum diode length for bipolar flow L^{BP}_{crit} is to first order simply a factor of 1.86 smaller than the minimum length without ions (i.e., $L^{BP}_{crit} = L_{crit}/1.86 = 2.6D/\beta^2$). This assumes that ion current is much less than the electron current. Also note that this last result only applies for $D \ll R$, because it has been shown recently that the factor of 1.86 increases with aspect ratio for cylindrical diodes (with the cathode radius larger than the anode radius)[12].

Extending these results to the relativistic regime and including ions in the analysis will require a numerical solution of Poisson's equation and is the subject for future work.

[1] C.D. Child, Phys. Rev. **32**, 492 (1911).
[2] I. Langmuir, Phys. Rev. **2**, 450 (1913).
[3] J.M. Creedon, J. Appl. Phys. **46**, 2946 (1975).
[4] A.E. Blaugrund, G. Cooperstein, and S.A. Goldstein, Phys. Fluids **20**, 1185 (1977).
[5] Y.Y. Lau, P.J. Christenson, and D. Chernin, Phys. Fluids **B5**, 4486 (1993).
[6] S.J. Stephanakis, D. Mosher, G. Cooperstein, J.R. Boller, J. Golden and S.A. Goldstein, Phys. Rev. Lett. <u>37</u>, 1543 (1976).
[7] S.B. Swanekamp, R.J Commisso, G. Cooperstein, P.F. Ottinger, and J.W. Schumer, Phys. Plasmas **7**, 5214 (2000).
[8] S.A. Goldstein and R. Lee, Phys. Rev. Lett. **35**, 1079 (1975).
[9] J.W. Poukey, Appl. Phys. Lett. **26**, 145 (1975).
[10] K.D. Bergeron, Appl. Phys. Lett. **28**, 306 (1976).
[11] I. Langmuir, Phys. Rev. **33**, 954 (1929).
[12] G. Cooperstein, J.R. Boller, R.J. Commisso, D.D. Hinshelwood, D. Mosher, P.F. Ottinger, J.W. Schumer, S.J. Stephanakis, S.B. Swanekamp, B.V. Weber, and F.C. Young, submitted to Phys. Plasma (2001).